

# A phonon-driven mechanism for an emergent and reversible chirality in crystals

Mauro Fava,<sup>1</sup> Emma McCabe,<sup>2</sup> Aldo H. Romero,<sup>3</sup> and Eric Bousquet<sup>1</sup>

<sup>1</sup>*Physique Théorique des Matériaux, QMAT, Université de Liège, B-4000 Sart-Tilman, Belgium*

<sup>2</sup>*Department of Physics, Durham University, South Road, Durham, DH1 3LE, U. K.*

<sup>3</sup>*Department of Physics and Astronomy, West Virginia University, Morgantown, WV 26505-6315, USA*

(Dated: May 22, 2024)

We demonstrate from first-principles calculations applied to the  $\text{K}_3\text{NiO}_2$  crystal that a structural phase transition from an achiral to a chiral phase can be mediated by a soft zone boundary phonon and that it can be controlled by pressure and epitaxial strain. Calculations in the presence of an electric field hint at a rich physics dominated by the competition between chirality, polar, and achiral distortions. Induced by the interaction between chiral, polar, and axial phonons, an optimal parameter window for the permanent reversal of chirality is observed.

Periodic solids are chiral if their structures are described by space groups containing only proper symmetry operations that map, for example, a right-handed coordinate system onto a right-handed one, and not onto a left-handed one (“operations of the first kind”), [1] otherwise they are achiral [2]. In recent years there has been a growing interest in investigating certain chiral effects (both in real- and spin-space) in crystals such as the Chiral Induced Spin Selectivity (CISS) and spin spirals [3, 4], polar [5] and magnetic skyrmions [6, 7], topological states [8, 9] and chiral phonons [10–12] to mention a few. Noticeably, the crystallization process fixes the chirality and associated properties in most of these instances. While the concept of spontaneous symmetry breaking has so far been a fertile ground for important discoveries in condensed matter physics [13], with phenomena such as ferroelectricity, magnetism, or superconductivity, to date, it has not been applied to study the possibility of chirality spontaneously emerging from an achiral inorganic solid phase. Nevertheless, a chiral irreducible representation (IRREP) or order parameter can be formally defined [14], so that a group-subgroup relationship of the type achiral  $\rightarrow$  chiral between two phases is a physical possibility [15]. Despite the recent experimental reports about the spontaneous formation of gyrotropic domains observed in certain materials [16–22] below a critical temperature, many questions remain to be answered about their physical origin and properties. At the most fundamental level, we know little about which mechanisms stabilize a chiral order. Furthermore, we do not know if an enantiomeric excess mediated by external fields or other parameters in a non-polar crystal and can be realized in the solid state.

In this work, we attempt to address these issues by exploring the achiral to chiral enantiomorphic phase transition observed in  $\text{K}_3\text{NiO}_2$  (KNO) [23]. Using symmetry analysis and density functional theory (DFT) calculations (see the Supplementary file [24] for technical details and references [25–33] there included), we show that a soft zone boundary phonon mode triggers the emergence of chirality in this material with four well-like shapes in the energy landscape. We then explore how this structural chiral energy surface is enhanced or reduced by

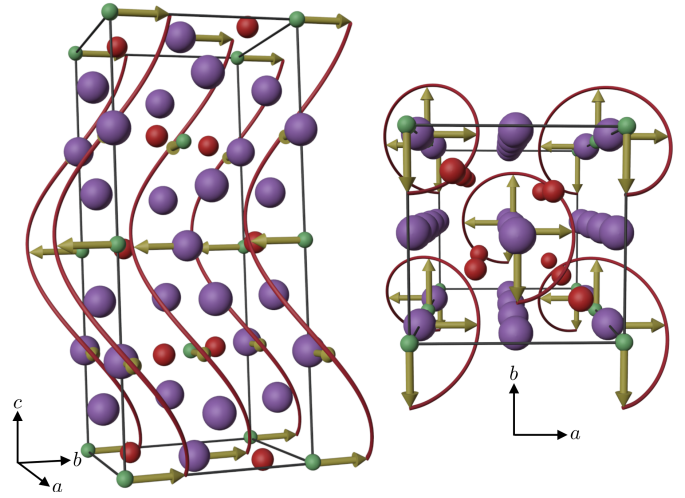


FIG. 1. Scheme of the soft chiral phonon distortion in  $\text{K}_3\text{NiO}_2$ . The purple, green, and red spheres correspond to K, Ni, and O atoms. The ions are in the  $P4_2/mnm$  configuration (unit cell doubled along the  $c$  axis), while the golden arrows and the red spirals represent the  $Z_4$  chiral  $P4_3(1)212$  displacement. The oxygen motion is not shown for clarity.

pressure or strain, and going further, we analyze how the chiral distortion can couple non-linearly with infrared (IR) and axial Raman active modes activated by an electric field. We prove that direct control over these polar and axial distortions is crucial to attain a permanent enantiomeric excess in a hysteresis-like manner and after said external field is removed. Our results can, therefore, be extrapolated to other chiral systems and allow us to explore strategies that may be adopted to optimize an enantiomeric excess in crystals via physical rather than possibly more invasive chemical procedures.

The high symmetry phase of KNO adopts an achiral tetragonal structure described by space group symmetry  $P4_2/mnm$  (no. 136). On cooling below  $\sim 423$  K, it undergoes a first-order phase transition to a low-temperature enantiomorphic phase of either  $P4_12_12$  (no. 92) or  $P4_32_12$  (no. 96) space groups [23]. Figure 1 shows the achiral high-temperature structure and illustrates the

chiral distortion. Our symmetry analysis reveals that the  $P4_2/mnm \rightarrow P4_12_12/P4_32_12$  non-invariant distortion  $|\delta\rangle$  decomposes into symmetry adapted modes (SAMs) as  $|\delta\rangle = a|Z_4\rangle + b|A_{1u}\rangle$ , where  $Z_4$  and  $A_{1u}$  are respectively the representation of the zone boundary ( $Z = 0, 0, 1/2$ ) mode (that triggers the instability, as we will see below) and of an associated  $\Gamma$ -point deformation which isotropy subgroup is  $P4_22_12$ . The  $Z_4$  mode involves the mostly in-plane motion of all the atom sites (although with larger K and O contributions in KNO) to form a spiral that preserves the 4-fold screw rotation of the parent phase. The  $A_{1u}$  pseudoscalar SAM describes a nonpolar K displacement along the  $c$  direction. As a consequence of  $|\delta\rangle$  the O - K - O bond angle becomes a little smaller than  $180^\circ$  whilst the  $\text{NiO}_2^{3-}$  units remain close to linear, consistent with experimental structure reports [23, 34, 35].

We perform our calculations with the collinear spins and the Hubbard-U correction ( $U = 4.2$  eV) on Ni ions (required to open a band gap) [24]. We calculate the phonon spectrum in the  $P4_2/mnm$  phase and identify a doubly degenerate soft mode at the Z point with frequency  $\omega_Z = 1.35i$  THz and  $Z_4$  irreducible representation, consistently with the aforementioned SAM analysis. Despite the proposals in the past of different mechanisms for the emergence of chirality from an achiral reference - such as Jahn-Teller [36] as in  $\text{CsCuClO}_3$ , or Peierls transitions [37] and orbital orders [38] as in the  $\text{MgTi}_2\text{O}_4$  compound - in KNO the driving force thus appears to be solely of phononic nature. While other soft modes (at  $\Gamma$ , X and M points [24]) are detected, the Z mode leads to the most stable low-symmetric configuration, as confirmed by the experiment. Since the  $Z_4$  soft boundary mode is doubly degenerate, we can build arbitrary linear combinations of eigenstates and calculate the energy as a function of their amplitude as illustrated in fig. 2. In particular, while the diagonal directions (a,a) and (a,-a) are associated with the realization of the  $P4_12_12$  and  $P4_32_12$  enantiomorphic domains, respectively, different settings lead to structures with different symmetries. In particular, the (a,0) and (0,b) directions produce degenerate orthorhombic phases with  $Cmcm$  (no. 63) symmetry, which are achiral and optically inactive, while arbitrary (a,b) (with  $a \neq 0$ ,  $b \neq 0$  and  $a \neq b$ ) combinations generate systems with  $C222_1$  symmetry. The free energy  $F$  - which includes the chiral  $\phi_Z = (\phi_a, \phi_b)$  SAMs amplitudes - thus reads  $F(\phi_Z) = \alpha|\phi_Z|^2 + \beta_1|\phi_Z|^4 + \beta_2(\phi_a^4 + \phi_b^4)$ .

The electronic density of states (DOS) near the Fermi level (see Fig. 3(a)) is mainly populated by weakly hybridized O-2p/Ni-3d valence and K-3d conduction states with the ground state in a low-spin configuration. We find the density of states to be negligibly affected by the phase transition [24], which also agrees with the rather nominal calculated Born effective charges [24] and possibly suggests a short-range interaction mechanism for the emergence of chirality, in agreement with its zone boundary nature [39]. Concerning the behavior under

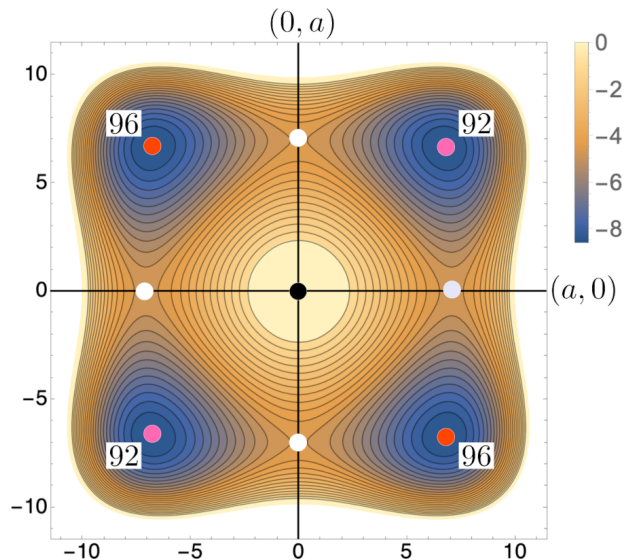


FIG. 2. Schematic 2D projection of the surface energy given by condensing the two-dimensional  $Z_4$  mode (amplitudes in arbitrary units). The central black circle corresponds to the high symmetry  $P4_2/mnm$  phase. The  $Cmcm$  (no. 63) energy minimum points are highlighted with white circles. Red and pink-filled circles indicate the degenerate ground state points in the  $P4_32_12$  (no. 96) and  $P4_12_12$  (no. 92) enantiomorphic phases, respectively.

mechanical perturbations, our results in Fig. 3(b)) show that even a tiny amount of hydrostatic pressure (above a value between 1.0 and 1.5 GPa) hardens the chiral mode and destroys the phase transition. This hardening under pressure may explain the observed decrease of the transition temperature upon replacing K with Rb or Cs, namely in  $\text{Rb}_3\text{NiO}_2$  ( $T_c = 390$  K) and  $\text{Cs}_3\text{NiO}_2$  (achiral at room temperature) [34]. Conversely, an even more nuanced effect can be observed in the presence of strain. Indeed, the  $Z_4$  mode is respectively hardened or softened if the applied in-plane  $\epsilon_{xx} = \epsilon_{yy}$  lattice deformation is tensile or compressive, as shown in Fig. 3(c). These results stem from a tension-compression asymmetry of the energy response in both the high and low symmetry phases. Nevertheless  $E(P4_2/mnm) > E(P4_1(3)2_12)$  always in the considered strain range ( $E$  is the energy, formula unit). Noticeably we find the  $\Gamma$  instability, which is polar ( $E_u$  representation) and comes from short-range forces (due to the non-anomalous Born charges [24]), to persist under tensile strain, with  $\Delta E(P4_2/mnm \rightarrow E_u) = -2.3$  meV upon  $\epsilon_{xx} = \epsilon_{yy} = 3\%$ . While this value lies higher than the corresponding chiral state energy, it is possible that ferroelectricity may coexist with chirality at this or at a larger magnitude of  $\epsilon_{xx} = \epsilon_{yy}$ . We leave this possibility open for future exploration.

*Handedness flipping.* Synthesized samples prepared by an azide-nitrate route resulted in racemic twinned crystals with approximately equal amounts of each enantiomorph (Flack parameter = 0.53) [23], illustrating the

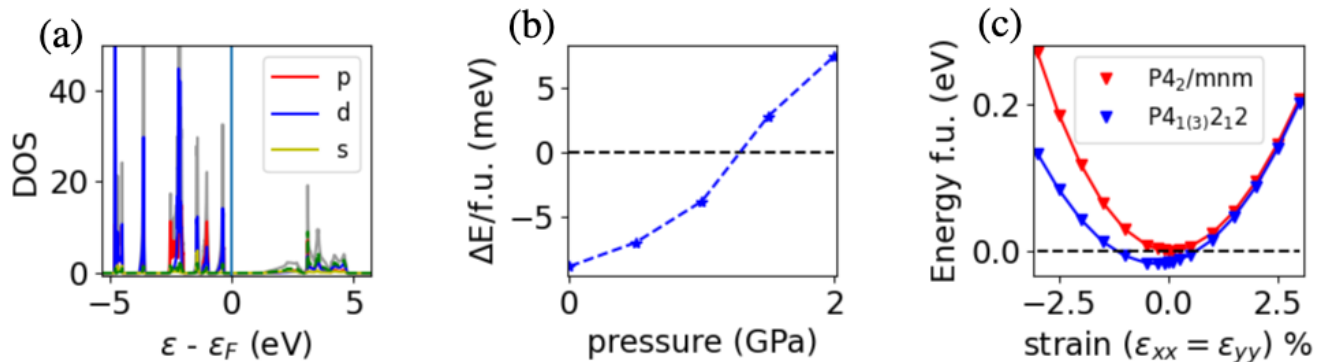


FIG. 3. (a) Partial electronic density of states near the Fermi level ( $P4_2/mnm$  phase). The dashed green curve represents K states and the grey curve the total DOS. (b) and (c)  $\Delta E(P4_2/mnm \rightarrow P4_{1(3)}2_12)$  behavior as a function of the hydrostatic pressure and epitaxial in-plane strain respectively.

difficulty of preparing enantiomerically pure samples. At the same time, the free energy expansion in presence of both chiral of zone-centre pseudoscalar amplitudes gets modified as  $F(\phi_Z, \phi_{A_{1u}}) = \alpha|\phi_Z|^2 + \beta_1|\phi_Z|^4 + \beta_2(\phi_a^4 + \phi_b^4) + \gamma(\phi_{A_{1u}})^2 + \delta\phi_a\phi_b\phi_{A_{1u}}$ , which shows that the chiral order parameter  $\phi_Z$  can couple trilinearly to the  $A_{1u}$  zone center mode. Therefore, any tensor  $\mathbf{T}$  containing the pseudoscalar irreducible representation can couple to the chiral  $Z_4$  mode as well through an invariant of the form  $\phi_a\phi_b\mathbf{T}$  and possibly induce control over the handedness of the system. One such tensor may be obtained by taking the product between vector ( $\mathbf{V} \equiv A_{2u} \oplus E_u$ ) and axial ( $\mathbf{A} \equiv A_{2g} \oplus E_g$ ) quantities. Indeed, the representation of this product can be decomposed into its irreducible components as  $\text{IRREP}(\mathbf{V} \otimes \mathbf{A}) = (A_{2u} \oplus E_u) \otimes (A_{2g} \oplus E_g) = 2A_{1u} \oplus 2E_u \oplus A_{2u} \oplus B_{1u} \oplus B_{2u}$  (note that both the  $A_{2u} \otimes A_{2g}$  and  $E_u \otimes E_g$  products contain  $A_{1u}$ ), thus revealing a pseudoscalar component.

We will now construct a model - based on the interaction between chiral, polar, and axial modes - that breaks the  $P4_12_12/P4_32_12$  degeneracy, realizes field-induced enantioselectivity and potentially creates a permanent enantiomeric excess. Applying an electric field results in the activation of polar in-plane ( $\phi_a^{IR}, \phi_b^{IR}$ ) and out-of-plane  $\phi_{A_{2u}}$  modes (with  $E_u$  and  $A_{2u}$  representations respectively). The axial Raman active modes ( $\phi_a^R, \phi_b^R$ ) with  $E_g$  representation can be switched on as well via trilinear  $\sim \phi_{A_{2u}}(\phi_a^R\phi_b^{IR} - \phi_b^R\phi_a^{IR})$  interaction, following a scheme analogous to that of orthorhombic  $\text{ErFeO}_3$  [40]. In the following we will explore how these field-induced distortions couple with the  $Z_4$  instability. Along with the always present biquadratic couplings, the following terms are allowed:

$$V_{\text{flip}} \propto \phi_a\phi_b(\phi_a^R\phi_b^{IR} + \phi_b^R\phi_a^{IR}) \quad (1)$$

and

$$V_{\text{Cmcm}} \propto (\phi_a^2 - \phi_b^2)\phi_a^{IR}\phi_b^{IR}. \quad (2)$$

While  $V_{\text{flip}}$  is an enantioselective mechanism that requires the activation of the  $E_g$  modes,  $V_{\text{Cmcm}}$  breaks the  $(\phi_a, 0)/(0, \phi_b)$  degeneracy of the  $Cmcm$  achiral distortion. It is interesting to check if the energy barrier that separates the right- and left-handed domains can in practice be overcome by  $V_{\text{flip}}$ . This would lead to a permanent enantiomeric excess (i.e. surviving the  $V_{\text{flip}} \rightarrow 0$  condition). To numerically test these ideas, we have extracted the relevant  $E_g$  and  $E_u$  modes via DFT structural relaxations in the presence of an electric field [41]. Importantly and since including collinear magnetism and the Hubbard-U interaction proves too numerically cumbersome in the presence of an electric field, we replace the K and Ni positions with Na and Au respectively to form a filled  $d$ -shell paramagnetic  $\text{Na}_3\text{AuO}_2$  (NAO) system with the same asymmetric unit of KNO and with a 2.1 eV DFT-computed band gap (without Hubbard correction). We note that although  $\text{Na}_3\text{AuO}_2$  has been shown experimentally to adopt a slightly different structure [42], our "toy model" (see the SI [24] for the details of its construction) provides a helpful approximation of KNO. We apply an electric field  $\mathcal{E} = 4.63 \times 10^4$  kV/m along the [1,1,1] direction to the high symmetry phase of  $\text{Na}_3\text{AuO}_2$ , perform a structural relaxation and extract the mixed polar-Raman distortion  $\equiv |\delta_{PR}|$ . Applied to the  $P4_2/mnm \rightarrow P4_{1(3)}2_12$  energy landscape, we observe that the overall effect of  $|\delta_{PR}|$  is to stabilize the  $Cmcm$  (0,b) distortion while hardening all other orthogonal  $Z_4$  directions ((a, $\pm$ a) and (a,0)) as a consequence of the effect of  $V_{\text{Cmcm}}$  [24]. Importantly, no energy difference between mirror-symmetric structures is detected. These features are also robust in the presence of an additional  $4/mmm \rightarrow mmm$  inducing compressive strain along the x-direction ( $\epsilon_{xx} = 1\%$  [24]). The lack of right/left splitting can be explained if one realises that  $V_{\text{flip}} \propto \epsilon_{xx}$  when  $\phi_{a(b)}^R \propto \phi_{A_{2u}}\phi_{a(b)}^{IR}$  [24]. Thus while the gyrotropic properties of KNO could be affected by the field, the absence of any  $P4_{1(3)}2_12 \rightarrow P4_2/mnm \rightarrow P4_{3(1)}2_12$  or

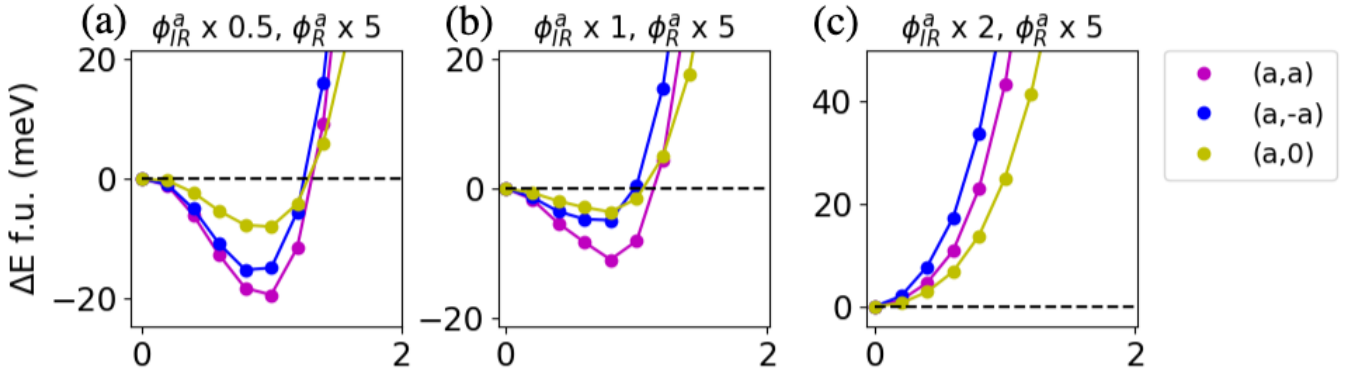


FIG. 4. DFT-evaluated energy landscape as a function of the  $\phi_Z$  amplitude in  $\text{Na}_3\text{AuO}_2$  and in the presence of additional in-plane polar  $E_u$  and axial  $E_g$  independent distortions (continuous segments are a guide to the eye). In this setting,  $V_{Cmcm} = 0$ . The  $E_g$  magnitude is fixed to be five times the value found via DFT via  $A_{2u}-E_u-E_g$  coupling (see main text), while the  $E_u$  amplitude is changed (0.5, 1 and 2 in figs. (b), (c) and (d) respectively). Fig.(c) shows the onset of a handedness flipping via crossing the  $P4_32_12 \rightarrow Cmcm \rightarrow P4_12_12$  energy barrier.

$P4_{1(3)}2_12 \rightarrow Cmcm \rightarrow P4_{3(1)}2_12$  crossing prevents the realization of a permanent enantiomeric excess. Instead of exploiting the aforementioned  $\sim \phi_{A_{2u}}(\phi_a^R \phi_b^{IR} - \phi_b^R \phi_a^{IR})$  nonlinear coupling in the presence of a constant bias along the  $[1,1,1]$  direction, we could use an axial external field - such as  $\nabla \times \mathcal{E}$  or  $\nabla \times \mathbf{u}$  [43, 44] (where  $\mathbf{u}$  defines an ionic displacement) - to switch the  $E_g$  modes on. Assuming we can activate  $E_u$  and  $E_g$  phonons along the  $(\phi_{IR}^a, 0)$  and  $(\phi_R^a, 0)$  directions respectively ( $\mathcal{E}_z$  along the  $c$  direction is set to zero), then  $V_{Cmcm} \rightarrow 0$  and the energy landscape may admit a sizable  $V_{\text{flip}}$  if the axial mode is large enough. For the sake of simplicity, we can assume to retain the polar-activated  $E_g$  mode, although admitting a linear scaling of its amplitude to mimic an axial conjugate field. The effect of this strategy is shown in Fig. 4(a,b,c). Fixing the  $E_g$  amplitude, a small polar mode as in Fig. 4(a) ( $\phi_{IR}^a \times 0.5$ ) breaks the degeneracy between mirror equivalent enantiomers but cannot result in the crossing of the  $P4_32_12 \rightarrow Cmcm \rightarrow P4_12_12$  barrier. On the other hand, increasing the polar scaling amplitude to 1 shows in Fig. 4(b) that there exists an optimal window for the realization of a permanent enantiomeric excess, as measured by the difference between  $P4_32_12$  and  $P4_12_12$  concerning the  $Cmcm$  distortion and  $P4_2/mnm$  reference. Finally, a larger  $E_u$  amplitude (e.g.  $\phi_{IR}^a \times 2$ ) has the effect of stabilizing the polar  $E_u$  state as reported in Fig. 4(c). Once the corresponding barrier has been crossed the system is expected to remain scalemic (e.g. non racemic) in zero-field conditions. The overall handedness of the system can therefore be inverted, by flipping the sign of the electric field direction and with a magnitude consistent with fig. 4(b), consistently with a mechanism that is analogous to a hysteresis process.

Realizing a reversible and controllable enantiomeric excess is therefore interlaced with the direct activation of polar and axial modes. The absence of a true conjugate field for the chiral order indicates that any handedness-

flipping interaction can activate achiral competing degrees of freedom as well (polar and  $Cmcm$  in this case). While it is possible for a phonon state to be polar and chiral at the same time [21], so that the chirality and associated gyrotropic properties can be controlled by an electric field [45, 46] as in the case of the  $\text{Pb}_5\text{Ge}_3\text{O}_{11}$  compound [22], this requires the axial mode to be invariant [22] which is not the case for enantiomorphic crystals such as KNO. In practice realizing an enantiomeric excess (or "chirality poling") could be achieved via chiral phonon-light coupling. By symmetry, the  $\mathbf{T}$  tensor coupling with the  $Z$  soft eigenmode may take the form of the so-called "Lipkin zilch" [43], which defines the chirality density -  $\rho_\chi = \frac{\epsilon_0}{2} \mathcal{E} \cdot (\nabla \times \mathcal{E}) + \frac{1}{2\mu_0} \mathcal{B} \cdot (\nabla \times \mathcal{B})$  - of a circularly polarised electromagnetic (EM) field. While no detailed study of an enantiomeric excess realized in the presence of a chiral phonon instability has been reported, the control over the phonon handedness in quartz has recently been obtained with the aid of circularly polarized X-rays[12].

*Conclusions.* In this work, we have explored the crystal chirality as a spontaneous order driven by a phonon instability with the  $\text{K}_3\text{NiO}_2$  compound as a model. In particular, a high-symmetry  $P4_2/mnm$  phase is lowered by a degenerate  $Z$  point soft mode to a pair of enantiomorphic structures with  $P4_12_12$  and  $P4_32_12$  symmetries. We have shown that an epitaxial strain can be used to either soften or harden the unstable mode, while a moderate hydrostatic pressure stabilizes the achiral  $P4_2/mnm$  phase. Finally, we have explored the possible realization of an enantiomeric excess in KNO mediated by a coupling between chiral, polar, and axial orders. Our findings highlight the rich phenomenology triggered by a static electric field, including a competition between chirality and orthorhombic ( $Cmcm$ ) phases and enantioselectivity. Nevertheless, we have numerically shown that the  $E_g$  modes, when activated via polar-polar-Raman coupling [40], can-

not efficiently lift the right/left degeneracy, so realizing a permanent handedness flipping could more likely be achieved by using an axial conjugate field (on top of an electric field) such as rotating EM fields or structural deformations. Additional theoretical and experimental analysis would be appealing to further understand our predictions on phonon-mediated chirality and the related new perspectives for enantioselectivity.

## ACKNOWLEDGEMENTS

Computational resources have been provided by the Consortium des Équipements de Calcul Intensif (CÉCI), funded by the Fonds de la Recherche Scientifique (F.R.S.-FNRS) under Grant No. 2.5020.11. MF & EB acknowledges FNRS for support and the PDR project CHRYSALID No.40003544. Work at West Virginia University was supported by the U.S. Department of Energy (DOE), Office of Science, Basic Energy Sciences (BES) under Award DE-SC0021375. This work used Bridges2 and Expanse at the Pittsburgh Supercomputer (Bridges2) and the San Diego Supercomputer Center (Expanse) through allocation DMR140031 from the Advanced Cyberinfrastructure Coordination Ecosystem: Services & Support (ACCESS) program, which National Science Foundation supports grants 2138259, 2138286, 2138307, 2137603, and 2138296.

- 
- [1] M. Nespolo, M. I. Aroyo, and B. Souvignier, Crystallographic shelves: space-group hierarchy explained, *Journal of Applied Crystallography* **51**, 1481 (2018).
- [2] H. Flack, Chiral and achiral crystal structures, *Helvetica Chimica Acta* **86**, 905 (2003).
- [3] S.-H. Yang, R. Naaman, Y. Paltiel, and S. S. P. Parkin, Chiral spintronics, *Nature Reviews Physics* **3**, 328 (2021).
- [4] F. Evers, A. Aharony, N. Bar-Gill, O. Entin-Wohlman, P. Hedegård, O. Hod, P. Jelinek, G. Kamieniarz, M. Lemesko, K. Michaeli, V. Mujica, R. Naaman, Y. Paltiel, S. Refaely-Abramson, O. Tal, J. Thijssen, M. Thoss, J. M. van Ruitenbeek, L. Venkataraman, D. H. Waldeck, B. Yan, and L. Kronik, Theory of chirality induced spin selectivity: Progress and challenges, *Advanced Materials* **34**, 2106629 (2022).
- [5] J. Junquera, Y. Nahas, S. Prokhorenko, L. Bellaiche, J. Íñiguez, D. G. Schlom, L.-Q. Chen, S. Salahuddin, D. A. Muller, L. W. Martin, and R. Ramesh, Topological phases in polar oxide nanostructures, *Rev. Mod. Phys.* **95**, 025001 (2023).
- [6] A. N. Bogdanov and U. K. Röfller, Chiral symmetry breaking in magnetic thin films and multilayers, *Phys. Rev. Lett.* **87**, 037203 (2001).
- [7] A. Fert, N. Reyren, and V. Cros, Magnetic skyrmions: advances in physics and potential applications, *Nature Reviews Materials* **2**, 17031 (2017).
- [8] G. Chang, B. J. Wieder, F. Schindler, D. S. Sanchez, I. Belopolski, S.-M. Huang, B. Singh, D. Wu, T.-R. Chang, T. Neupert, S.-Y. Xu, H. Lin, and M. Z. Hasan, Topological quantum properties of chiral crystals, *Nature Materials* **17**, 978 (2018).
- [9] N. B. M. Schröter, S. Stolz, K. Manna, F. de Juan, M. G. Vergniory, J. A. Krieger, D. Pei, T. Schmitt, P. Dudin, T. K. Kim, C. Cacho, B. Bradlyn, H. Bornmann, M. Schmidt, R. Widmer, V. N. Strocov, and C. Felser, Observation and control of maximal chern numbers in a chiral topological semimetal, *Science* **369**, 179 (2020).
- [10] L. Zhang and Q. Niu, Chiral phonons at high-symmetry points in monolayer hexagonal lattices, *Phys. Rev. Lett.* **115**, 115502 (2015).
- [11] K. Ishito, H. Mao, Y. Kousaka, Y. Togawa, S. Iwasaki, T. Zhang, S. Murakami, J.-i. Kishine, and T. Satoh, Truly chiral phonons in  $\alpha$ -hgs, *Nature Physics* **19**, 35 (2023).
- [12] H. Ueda, M. García-Fernández, S. Agrestini, C. P. Romao, J. van den Brink, N. A. Spaldin, K.-J. Zhou, and U. Staub, Chiral phonons in quartz probed by x-rays, *Nature* **618**, 946 (2023).
- [13] A. Beekman, L. Rademaker, and J. van Wezel, An introduction to spontaneous symmetry breaking, SciPost Physics Lecture Notes , 011 (2019).
- [14] J. Hlinka, Eight types of symmetrically distinct vectorlike physical quantities, *Phys. Rev. Lett.* **113**, 165502 (2014).
- [15] K. C. Erb and J. Hlinka, Symmetry guide to chiroaxial transitions, *Phase Transitions* **91**, 953 (2018).
- [16] T. Hayashida, K. Kimura, D. Urushihara, T. Asaka, and T. Kimura, Observation of ferrochiral transition induced by an antiferroaxial ordering of antipolar structural units in  $\text{Ba}(\text{TiO})\text{Cu}_4(\text{PO}_4)_4$ , *J. Am. Chem. Soc.* **143**, 3638 (2021).
- [17] K. Kimura, M. Sera, and T. Kimura, A2+ cation control of chiral domain formation in  $\text{A}(\text{TiO})\text{Cu}_4(\text{PO}_4)_4$  (A = Ba, Sr), *Inorganic Chemistry* **55**, 1002 (2016).
- [18] P. Huang, Z. Xia, X. Gao, J. M. Rondinelli, X. Zhang, H. Zhang, K. R. Poeppelmeier, and A. Zunger, Ferrochiral compounds with potentially switchable dresselhaus spin splitting, *Phys. Rev. B* **102**, 235127 (2020).
- [19] T. Hayashida, K. Kimura, D. Urushihara, T. Asaka, and T. Kimura, Observation of ferrochiral transition induced by an antiferroaxial ordering of antipolar structural units in  $\text{ba}(\text{tio})\text{cu}_4(\text{po}_4)_4$ , *Journal of the American Chemical Society* **143**, 3638 (2021).
- [20] T. Hayashida, K. Kimura, and T. Kimura, Switching crystallographic chirality in  $\text{ba}(\text{tio})\text{cu}_4(\text{po}_4)_4$  by laser irradiation, *The Journal of Physical Chemistry Letters* **13**, 3857 (2022).
- [21] M. Fava, W. Lafargue-Dit-Hauret, A. H. Romero, and E. Bousquet, Ferroelectricity and chirality in the  $\text{pb}_5\text{ge}_3\text{o}_{11}$  crystal, *Phys. Rev. B* **109**, 024113 (2024).
- [22] M. Fava, W. Lafargue-Dit-Hauret, A. H. Romero, and E. Bousquet, Ferroelectricity and chirality in the  $\text{pb}_5\text{ge}_3\text{o}_{11}$  crystal (2023).
- [23] K. Đuriš, U. Müller, and M. Jansen, K3nio2 revisited, phase transition and crystal structure refinement, *Zeitschrift für anorganische und allgemeine Chemie* **638**, 737 (2012).
- [24] Supplemental materials, [Supplementalmaterials,URL\\_will\\_be\\_inserted\\_by\\_publisher](#) (2023).
- [25] G. Kresse and D. Joubert, From ultrasoft pseudopotentials to the projector augmented-wave method, *Phys. Rev. B* **59**, 1758 (1999).

- [26] J. P. Perdew, K. Burke, and M. Ernzerhof, Generalized gradient approximation made simple, *Phys. Rev. Lett.* **77**, 3865 (1996).
- [27] S. L. Dudarev, G. A. Botton, S. Y. Savrasov, C. J. Humphreys, and A. P. Sutton, Electron-energy-loss spectra and the structural stability of nickel oxide: An lsd+u study, *Phys. Rev. B* **57**, 1505 (1998).
- [28] M. Cococcioni and S. de Gironcoli, Linear response approach to the calculation of the effective interaction parameters in the LDA + U method, *Phys. Rev. B* **71**, 035105 (2005).
- [29] H. T. Stokes, D. M. Hatch, B. J. Campbell, and D. E. Tanner, Isodisplace: a web-based tool for exploring structural distortions, *Journal of Applied Crystallography* **39**, 607 (2006), <https://onlinelibrary.wiley.com/doi/pdf/10.1107/S0021889806014075>
- [30] D. Orobengoa, C. Capillas, M. I. Aroyo, and J. M. Perez-Mato, *AMPLIMODES*: symmetry-mode analysis on the Bilbao Crystallographic Server, *J. Appl. Crystallogr.* **42**, 820 (2009).
- [31] X. Gonze, B. Amadon, G. Antonius, F. Arnardi, L. Baguet, J.-M. Beuken, J. Bieder, F. Bottin, J. Bouchet, E. Bousquet, N. Brouwer, F. Bruneval, G. Brunin, T. Cavignac, J.-B. Charraud, W. Chen, M. Côté, S. Cottenier, J. Denier, G. Geneste, P. Ghosez, M. Giantomassi, Y. Gillet, O. Gingras, D. R. Hamann, G. Hautier, X. He, N. Helbig, N. Holzwarth, Y. Jia, F. Jollet, W. Lafargue-Dit-Hauret, K. Lejaeghere, M. A. Marques, A. Martin, C. Martins, H. P. Miranda, F. Naccarato, K. Persson, G. Petretto, V. Planes, Y. Pouillon, S. Prokhorenko, F. Ricci, G.-M. Rignanese, A. H. Romero, M. M. Schmitt, M. Torrent, M. J. van Setten, B. Van Troeye, M. J. Verstraete, G. Zerah, and J. W. Zwanziger, The abinitproject: Impact, environment and recent developments, *Computer Physics Communications* **248**, 107042 (2020).
- [32] M. Van Setten, M. Giantomassi, E. Bousquet, M. J. Verstraete, D. R. Hamann, X. Gonze, and G.-M. Rignanese, The pseudodojo: Training and grading a 85 element optimized norm-conserving pseudopotential table, *Comput. Phys. Commun.* **226**, 39 (2018).
- [33] G. Wagner and R. Hoppe, Oxydation intermetallischerphasen: Na<sub>3</sub>[auo<sub>2</sub>] aus naau und na<sub>2</sub>o<sub>2</sub>, *Zeitschrift für anorganische und allgemeine Chemie* **549**, 26 (1987).
- [34] K. Durisi, O. V. Magdysyuk, and M. Jansen, Syntheses, structures and magnetic properties of the alkali oxonickelates(i) a<sub>3</sub>nio<sub>2</sub> (aÅ = Å k, rb, cs), *Solid State Sciences* **14**, 1399 (2012).
- [35] A. Moeller, M. A. Hitchman, E. Krausz, and R. Hoppe, Synthesis, crystal structure and physical properties of kna<sub>2</sub>[nio<sub>2</sub>] and k<sub>3</sub>[nio<sub>2</sub>] containing "linear" [nio<sub>2</sub>]<sup>3-</sup> anions, *Inorganic Chemistry* **34**, 2684 (1995).
- [36] S. Hirotsu, Jahn-teller induced phase transition in CsCuCl<sub>3</sub>: structural phase transition with helical atomic displacements, *J. Phys. C: Solid State Phys.* **10**, 967 (1977).
- [37] D. I. Khomskii and T. Mizokawa, Orbital induced peierls state in spinels, *Phys. Rev. Lett.* **94**, 156402 (2005).
- [38] S. Di Matteo, G. Jackeli, C. Lacroix, and N. B. Perkins, Valence-bond crystal in a pyrochlore antiferromagnet with orbital degeneracy, *Phys. Rev. Lett.* **93**, 077208 (2004).
- [39] G. A. Samara, T. Sakudo, and K. Yoshimitsu, Important generalization concerning the role of competing forces in displacive phase transitions, *Phys. Rev. Lett.* **35**, 1767 (1975).
- [40] D. M. Juraschek, M. Fechner, and N. A. Spaldin, Ultrafast structure switching through nonlinear phononics, *Phys. Rev. Lett.* **118**, 054101 (2017).
- [41] I. Souza, J. Íñiguez, and D. Vanderbilt, First-principles approach to insulators in finite electric fields, *Phys. Rev. Lett.* **89**, 117602 (2002).
- [42] G. Wagner and R. Hoppe, Oxydation intermetallischerphasen: Na<sub>3</sub>[auo<sub>2</sub>] aus naau und na<sub>2</sub>o<sub>2</sub>, *Zeitschrift für anorganische und allgemeine Chemie* **549**, 26 (1987), <https://onlinelibrary.wiley.com/doi/pdf/10.1002/zaac.19875490604>.
- [43] Y. Tang and A. E. Cohen, Optical chirality and its interaction with matter, *Phys. Rev. Lett.* **104**, 163901 (2010).
- [44] R. Oiwa and H. Kusunose, Rotation, electric-field responses, and absolute enantioselection in chiral crystals, *Phys. Rev. Lett.* **129**, 116401 (2022).
- [45] H. Iwasaki, K. Sugii, T. Yamada, and N. Niizeki, 5pbo [center-dot] 3geo[<sub>sub</sub> 2] crystal; a new ferroelectric, *Appl. Phys. Lett.* **18**, 444 (1971).
- [46] H. Iwasaki, S. Miyazawa, H. Koizumi, K. Sugii, and N. Niizeki, Ferroelectric and optical properties of pb<sub>5</sub>ge<sub>3</sub>o<sub>11</sub> and its isomorphous compound pb<sub>5</sub>ge<sub>2</sub>sio<sub>11</sub>, *J. Appl. Phys.* **43**, 4907 (1972).